

Review

Open Access



Chapter: imaging of atrial and ventricular septal defects

Santosh C. Uppu

Children's Heart Institute, McGovern Medical School, University of Texas Health Science Center at Houston, Houston, TX 77030, USA.

Correspondence to: Assoc. Prof. Santosh C. Uppu, Pediatrics, Internal Medicine and Radiology Children's Memorial Hermann Hospital McGovern Medical School at UT Health Houston, 6410 Fannin Street, Suite 425, Houston, TX 77030, USA.
E-mail: Santosh.C.Uppu@uth.tmc.edu

How to cite this article: Uppu SC. Chapter: imaging of atrial and ventricular septal defects. *Vessel Plus* 2021;6:21.
<https://dx.doi.org/10.20517/2574-1209.2021.101>

Received: 15 Jul 2021 **First Decision:** 13 Sep 2021 **Revised:** 30 Sep 2021 **Accepted:** 19 Oct 2021 **Published:** 8 Apr 2022

Academic Editors: P Syamasundar Rao, Francesco Nappi **Copy Editor:** Yue-Yue Zhang **Production Editor:** Yue-Yue Zhang

Abstract

Septal defects together account for the majority of the congenital heart defects (CHD); these can occur in isolation or associated with other CHDs. Hemodynamic manifestations are dependent upon the size, location, and the number of the defects, along with the associated lesions. For example, atrial septal defects result in the right ventricular volume overload, whereas the ventricular septal defect (VSD) results in the left heart volume overload. Knowledge of septal anatomy is crucial to understanding these lesions, their hemodynamic significance, and thus better plan management, including interventions. Noninvasive imaging of simple septal defects by various modalities will be reviewed; atrioventricular septal defects, anomalous pulmonary venous connections, patent ductus arteriosus, and complex cardiac conditions with VSD will not be discussed in this chapter.

Keywords: Atrial septal defect, ventricular septal defect, echocardiography, cardiac MRI, cardiac CT, congenital heart defects

INTRODUCTION

Atrial and ventricular septal defects constitute the majority of the congenital heart defects (CHDs); these can occur in isolation or associated with other CHDs. A recent systematic review has reported the prevalence of atrial and ventricular septal defects as 0.144 and 0.307 per 100 live births, respectively,



© The Author(s) 2022. **Open Access** This article is licensed under a Creative Commons Attribution 4.0 International License (<https://creativecommons.org/licenses/by/4.0/>), which permits unrestricted use, sharing, adaptation, distribution and reproduction in any medium or format, for any purpose, even commercially, as long as you give appropriate credit to the original author(s) and the source, provide a link to the Creative Commons license, and indicate if changes were made.



accounting for about 15% and 35% of all congenital heart defects^[1]. In the absence of elevated pulmonary vascular resistance (PVR), they result in left to right shunting, thus are part of acyanotic CHDs. Hemodynamic manifestations are dependent upon the size, location, and number of defects. Relative ventricular compliance drives the degree of shunting across an atrial septal defects (ASD), whereas the PVR is crucial for shunting across the VSD^[2-7]. The pathophysiology of VSD is discussed elsewhere in this book, and its general principles are applicable to ASD as well. In summary, hemodynamically significant ASDs with pulmonary to systemic blood flow ratio (Q_p/Q_s) > 1.5 result in the right ventricular volume overload^[8], whereas the hemodynamically significant VSDs result in left heart volume overload^[9]. Patients with smaller shunt lesions are usually asymptomatic and may incidentally be diagnosed later in life^[10]. Small ASD and VSDs may spontaneously close in early life. Knowledge of the septal anatomy, identifying associated lesions are crucial while planning their management^[8,9,11]. This chapter will focus on noninvasive imaging before, during, and post intervention.

ANATOMY OF ATRIAL SEPTAL DEFECTS

Atrial septum forms around the 4th week with septum primum growing towards the atrioventricular (AV) canal from the roof of the common atrium; the resultant communication is ostium primum. As the endocardial cushions fuse and join the septum primum, apoptosis at the superior margin of the septum primum results in the formation of an ostium secundum atrial communication. A new septal infolding appears on the right atrial aspect of the ostium secundum that ultimately becomes septum secundum. As the septum secundum elongates, it becomes a stiff limbus of fossa ovalis. The septum primum remains thin and has a flap valve mechanism that redirects oxygen-rich inferior vena caval blood towards the left atrium across the patent foramen ovale. Postnatally increasing left atrial pressure closes the atrial septum^[12,13]. During the 5th week, the left vitelline veins regress along with the left horn of sinus venosus as the right vitelline veins become dominant. By 10 weeks, the left cardinal vein regresses, and the left sinus horn is represented postnatally by the coronary sinus and oblique vein of the left atrium that empty into the right atrium^[12,14,15].

Atrial septal defects are classified into:

Ostium secundum atrial septal defect

Ostium secundum ASD (OS ASD) are the most common ASDs that result from a defect within the fossa ovalis or septum primum. As a result, they are centrally located within the atrial septum and are thus away from vena cavae, right pulmonary veins, coronary sinus or the AV valves [Figures 1 and 2].

OS ASD can be single or multiple with fenestrations in the septum primum. Large OS ASDs can rarely result in deficiency of limbus of the fossa ovalis, thus resulting in the superior location of the ASD closer to the superior vena caval (SVC) entrance and are called high OS ASD. Inferior vena cava (IVC) confluent OS ASD results in the deficiency of the septum primum all the way to the IVC entrance^[2,7,16] [Figure 3].

Ostium primum atrial septal defect

Ostium primum ASD results from a defect within the endocardial cushion portion of the atrial septum at the cardiac crux between the fossa ovalis and the AV valve [Figure 4]. These defects account for about 10% of the ASDs. It is a form of endocardial cushion defect and is often associated with AV valve abnormalities^[2,4].

Sinus venosus defect

Sinus venosus defects (SVD) are not true ASDs, and they account for 5%-10% of atrial septal

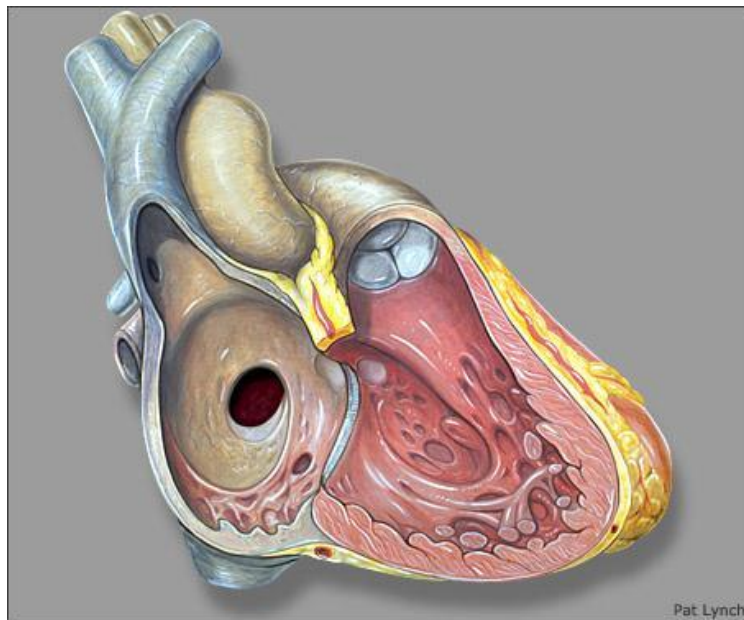


Figure 1. Image showing ostium secundum atrial septal defect as a defect within the fossa ovalis.

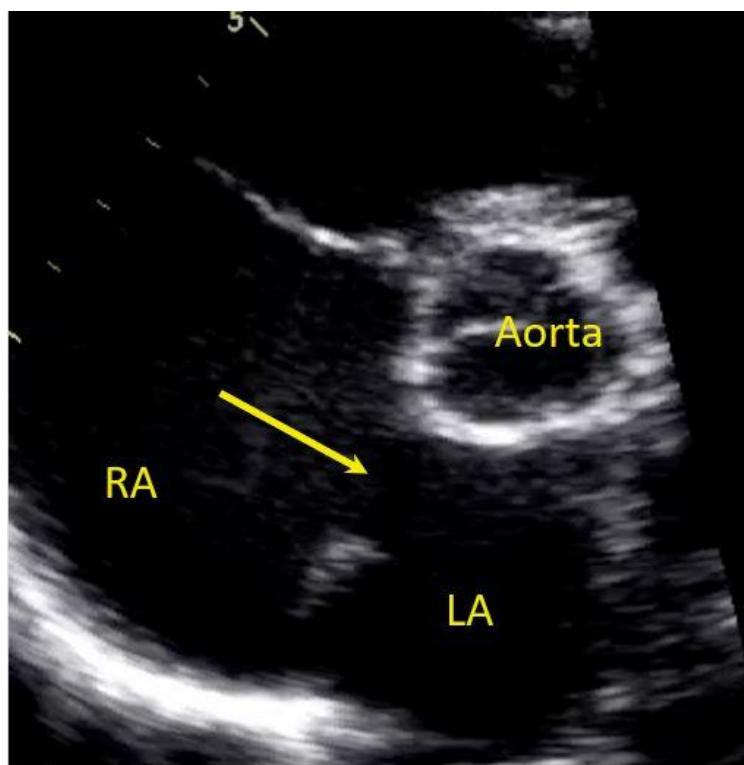


Figure 2. Still image from a trans-thoracic echocardiogram in parasternal short-axis view in a teenager showing a large ostium secundum atrial septal defect with deficient retroaortic rim (yellow arrow). RA: Right atrium; LA: left atrium.

communication defects. SVDs result from incomplete incorporation of the right horn of sinus venosus into the right atrium (RA) along with abnormal septum secundum formation. As a result, commonly, there is

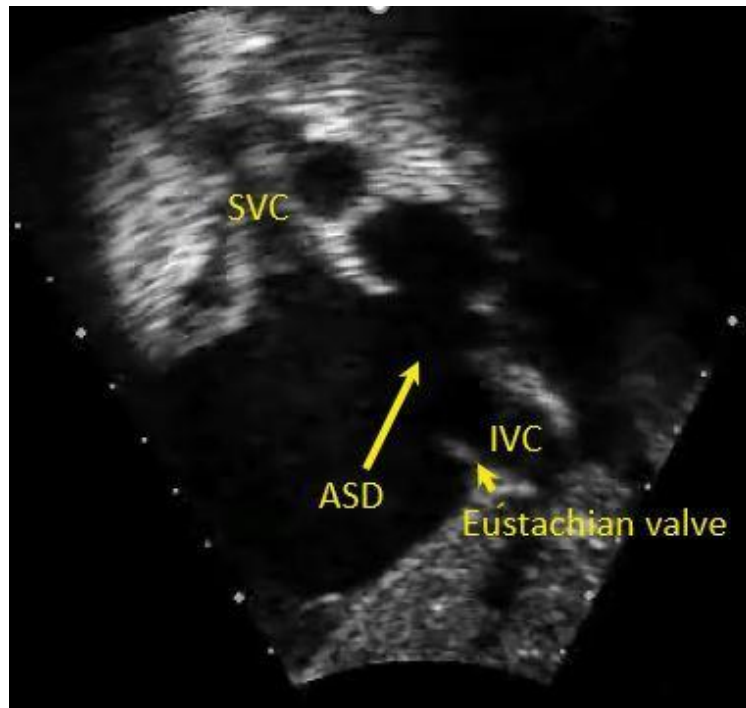


Figure 3. Still image from a trans-thoracic echocardiogram in subcostal short-axis view in a teenager showing a large IVC confluent ostium secundum atrial septal defect (long yellow arrow), notice the prominent Eustachian valve (short yellow arrow). SVC: Superior vena cava; IVC: inferior vena cava; ASD: atrial septal defect.

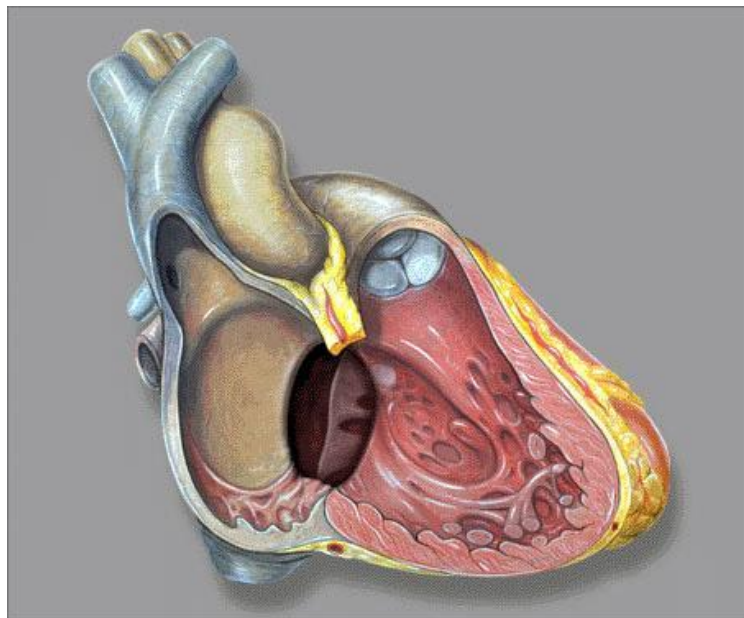


Figure 4. Image showing the location of the ostium primum atrial septal defect at the crux of the heart along with inlet ventricular septal defect.

communication between the right-sided pulmonary veins and the cardiac end of the SVC or the superior portion of the RA in SVC type SVD. Rarely there is a deficiency of wall separating the right middle/lower

pulmonary veins and lower portion of the RA in IVC type SVD [Figure 5]. The pulmonary venous orifice to the left atrium (LA) is commonly preserved, the pulmonary venous flow destined to LA empties into the right atrium, there is an additional left to right shunting across the pulmonary venous orifice into the RA across the SVC, as such there is significant right heart dilatation that is out of proportion to the size of the defect. SVC type SVD is often associated with partial anomalous pulmonary venous connections^[4,6,7,17].

Coronary sinus defect

Coronary sinus defect (CSD) is rare and results from incomplete fusion of the left horn of sinus venosus with the septum primum. CSDs are almost always associated with Left SVC draining into the LA results from the partial or complete unroofing of the coronary sinus (CS) where the wall separating the CS from the left atrium may be partially or completely deficient, there is a coronary sinus opening in the right atrium that functions as an atrial septal communication (Raghib syndrome)^[14,18,19] [Figure 6]. This results in desaturated blood entering the systemic circulation and cyanosis. If the degree of cyanosis is not clinically obvious, these patients can present with polycythemia, paradoxical emboli, stroke, or brain abscess^[20].

IMAGING ATRIAL SEPTAL DEFECT

Knowledge of atrial septal anatomy is crucial to understanding and visualizing the ASDs. Given the complex three-dimensional (3D) structure of the atrial septum, one has to image it from multiple views to have a global perspective. Two-dimensional (2D) transthoracic echocardiography (TTE) is still the diagnostic modality of choice and often helps with the diagnosis. In subjects with good acoustic windows, the atrial septum can be better evaluated from the subcostal and high right parasternal windows, where the atrial septum is profiled perpendicular to the ultrasound beam. Thus false dropouts seen from traditional apical views can be avoided. Slow, long sweeps help with better visualization of the entire septum. Identifying the location, size, rims, the number of defects, surrounding structures, and evaluation for possible associated lesions help tailor the management plan^[7,21].

Three-dimensional echocardiography is being utilized more frequently given the immediate access to the technology along with fast post-processing capability of the 3D datasets that helps with better visualization of the defect in relation to its surroundings and check rims and device placement^[22,23] [Figure 7]. However, 3D TTE technology has the same setbacks as traditional 2D echocardiography as they both require good acoustic windows.

In patients with poor acoustic windows, one can consider transesophageal echocardiography (TEE) [Figure 8] or alternative imaging such as cardiac magnetic resonance imaging (CMR)^[24].

Patients with OS ASD who are deemed to be potential candidates for device closure need proper measurement of the defects from all the imaging views^[25,26]. In addition, it is also important to measure the rims, total septal length, which helps to choose the device. This can be achieved pre-procedure or at the time of the intervention using TEE^[8,27,28].

OS ASDs are better visualized from the parasternal short axis, subcostal short and long axis, and high right parasternal windows. Therefore, it is important to notify the operator of a prominent Eustachian valve in patients undergoing surgical closure, especially in those with IVC confluent OS ASD, so that it is not mistaken for the inferior rim of the ASD^[29-31].

Cross-sectional imaging with CMR and cardiac computed tomography (CT) can be considered in a select group of patients where echocardiography is suboptimal or vascular/venous anomalies are suspected as they

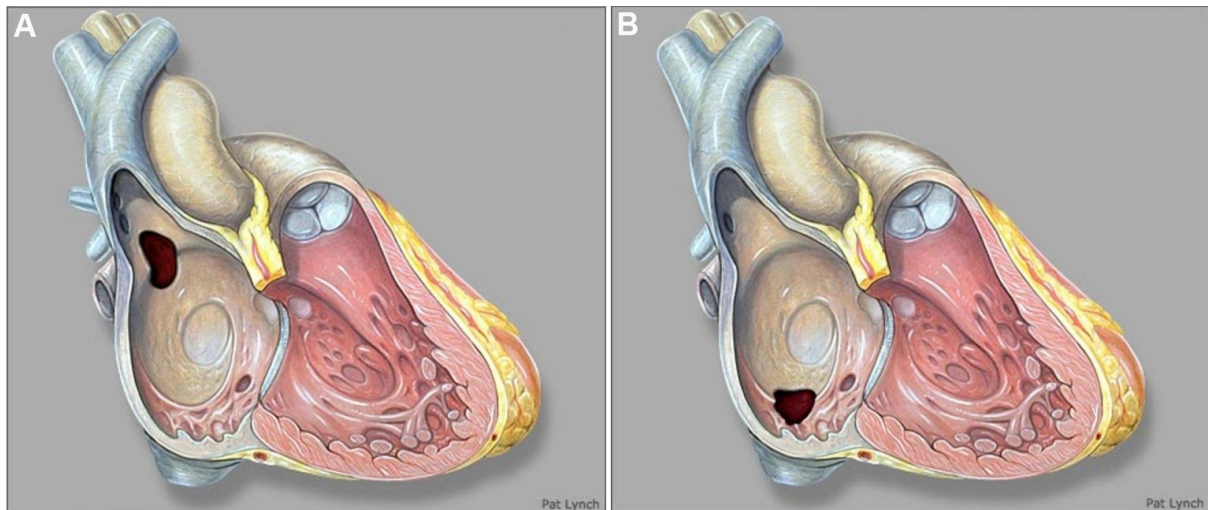


Figure 5. Images showing superior vena caval (A) and inferior vena caval type (B) of sinus venosus defects, respectively.

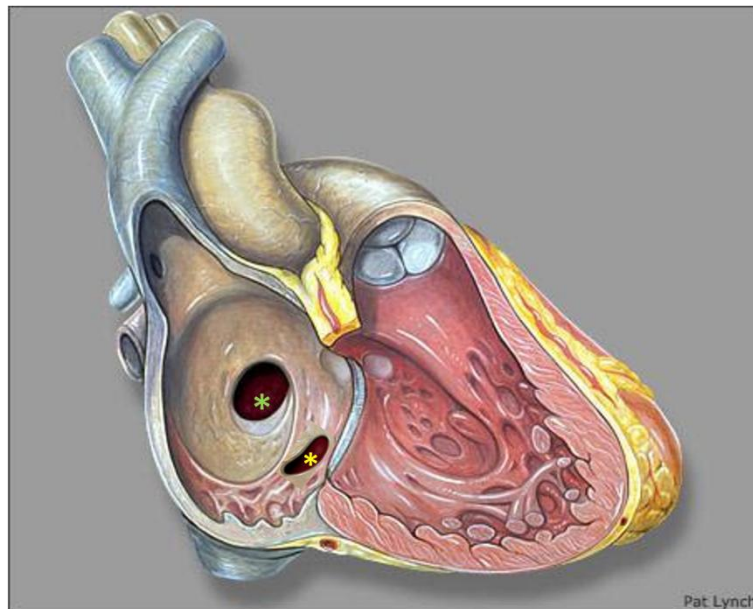


Figure 6. Image showing the location of the coronary sinus defect (yellow asterisk) in relation to ostium secundum ASD (green asterisk). ASD: Atrial septal defect.

provide superior 3D datasets^[10,13,23,24]. Furthermore, CMR provides additional data by quantifying ventricular volumes and obtaining Qp/Qs using phase contrast techniques. In addition, datasets from 3D echo, CMR, and CT can be fused with fluoroscopy to reduce radiation exposure and the time for intervention^[32].

SVDs are better visualized from the subcostal and high right parasternal windows [Figures 9 and 10].

Given the high association of partial anomalous pulmonary venous connections, one has to consider a CMR or CT prior to planned surgical intervention [Figures 11-13]. Transcatheter correction of the SVC type SVD using a covered stent is feasible in a select group of patients. Cross-sectional imaging, either with CMR or CT, along with simulation using virtual 3D models, is essential for careful patient selection^[9,33].

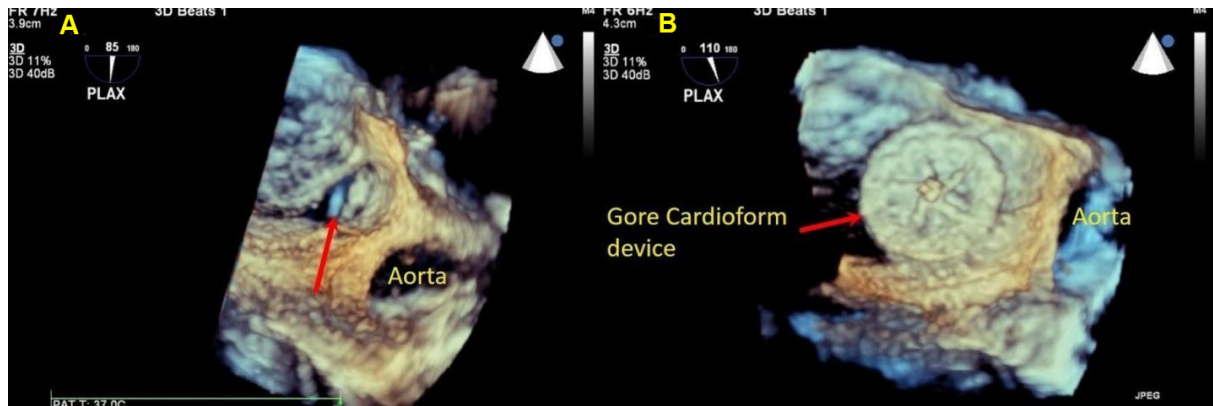


Figure 7. Still three-dimensional images from a trans-esophageal echocardiogram performed during device placement in a teenager, panel A shows an ostium secundum atrial septal defect with deficient retroaortic rim (red arrow). Panel B shows a successfully deployed GORE® CARDIOFORM ASD occluder in the satisfactory position seen in its entirety (red arrow). ASD: Atrial septal defect.

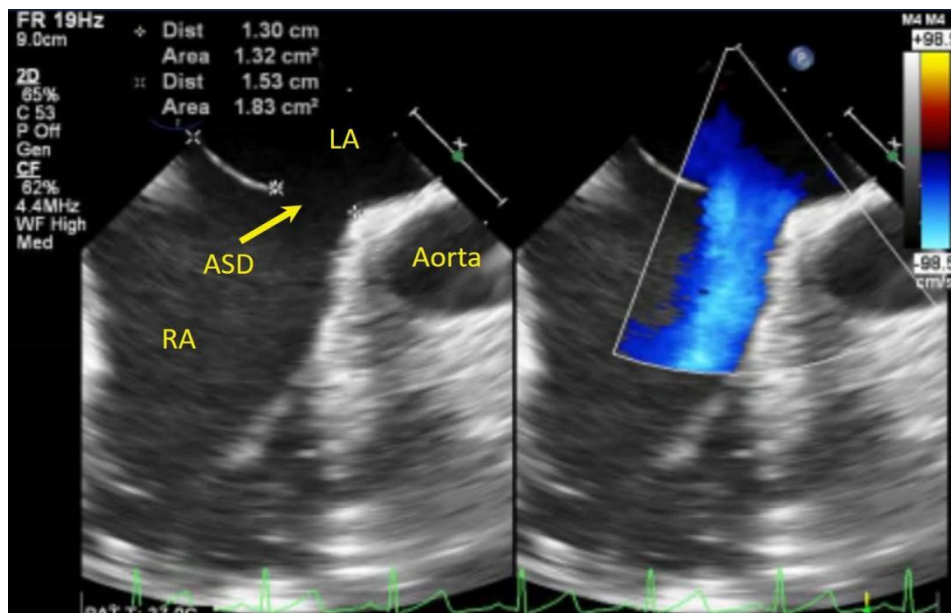


Figure 8. Still image from a trans-esophageal echocardiogram in a young adult showing an ostium secundum atrial septal defect with deficient retroaortic rim (yellow arrow), color flow mapping shows left to right shunting across the defect. RA: Right atrium; LA: left atrium; ASD: atrial septal defect.

CSDs are difficult to visualize by traditional views. It is important to perform echo sweeps to image the atrial septum carefully around the location of the CS ostium, and TEE may help in those with difficult windows [Figure 14]. Contrast injection in the left arm in patients with suspected CSD with partially or completely unroofed CS can help with identification^[7].

ANATOMY OF VENTRICULAR SEPTAL DEFECTS

The ventricular septal formation is a complex process that begins at the end of the 4th week. Therefore, a detailed description of the ventricular septal formation, including genetic basis, is beyond the scope of this chapter^[3,5,12,34,35].

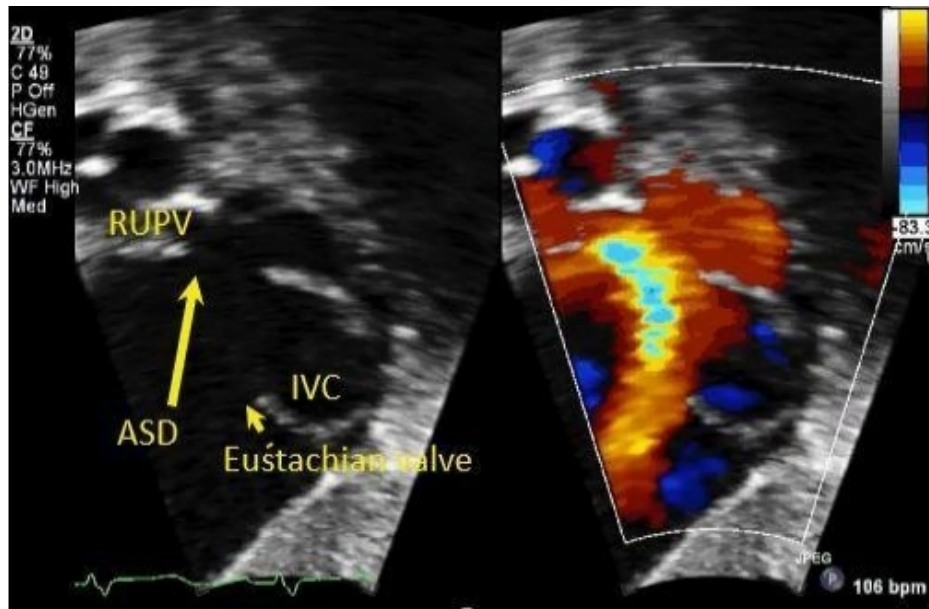


Figure 9. Still color Doppler image from a trans-thoracic echocardiogram in a young child in subcostal short-axis view showing a superior vena caval type sinus venosus defect (long yellow arrow). Flow from the right upper pulmonary vein (RUPV) is seen emptying into the right atrium. There is a prominent Eustachian valve (short yellow arrow) seen anterior to the inferior vena caval entrance (IVC).

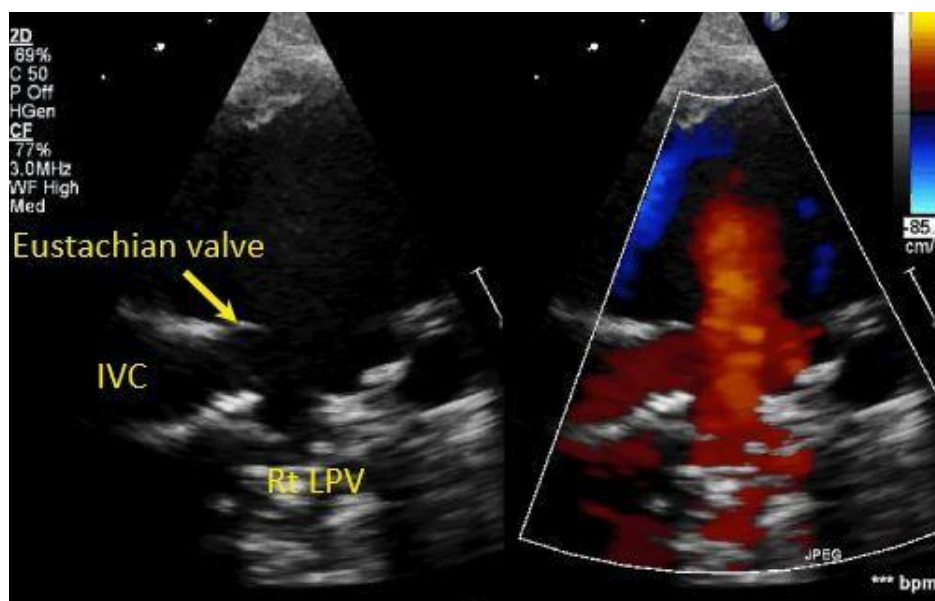


Figure 10. Still color Doppler image from a trans-thoracic echocardiogram in a young child in high right parasternal short-axis view showing an inferior vena caval type sinus venosus defect behind the prominent Eustachian valve (short yellow arrow). Flow from the right lower pulmonary vein (Rt LPV) is seen emptying into the right atrium adjacent to the entrance of the inferior vena caval entrance (IVC).

There is extensive controversy around the nomenclature of the VSDs. The International Society for Nomenclature of Paediatric and Congenital Heart Disease has tried to address the issue by proposing a classification scheme that has been incorporated in the International Classification of Diseases-11th iteration^[11,36].

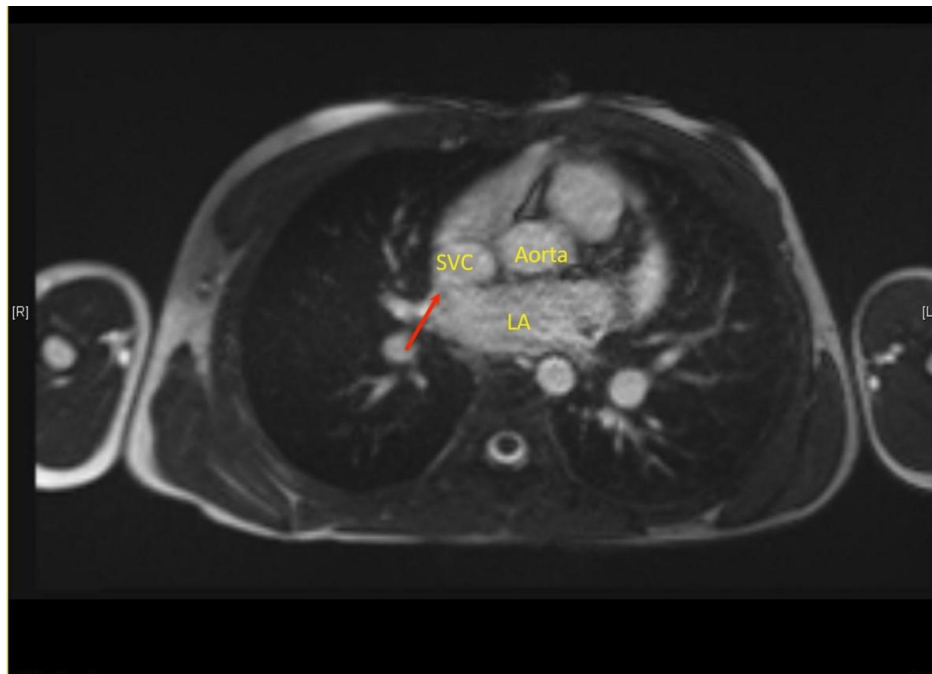


Figure 11. Still axial image in a young adult from a cine cardiac magnetic resonance imaging showing absent wall between the superior vena cava (SVC) and the right upper pulmonary venous entrance (red arrow) in a superior vena caval type sinus venosus defect. LA: Left atrium.

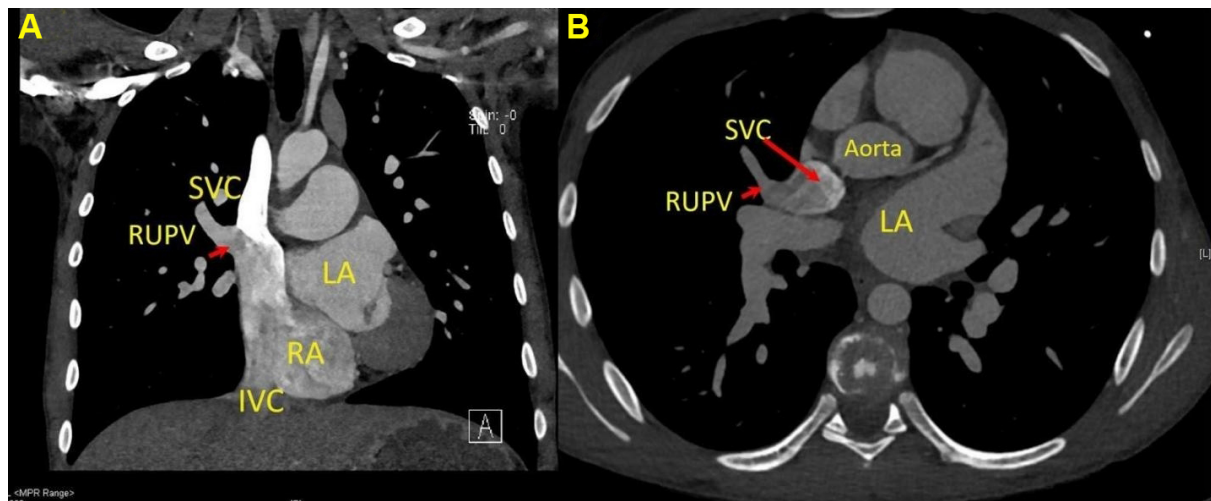


Figure 12. Panel A shows a still coronal image from a cardiac computational tomography in a young adult imaging showing the partial anomalous connection of the right upper pulmonary vein (RUPV) to the superior vena cava (SVC) (short red arrow). Panel B shows a still axial image with the partial anomalous connection of the RUPV to the SVC. LA: Left atrium; RA: right atrium; IVC: inferior vena cava.

Ventricular septal defects are broadly classified as:

Perimembranous ventricular septal defect

Also called the central VSD, they account for the majority of the VSDs. These defects are found in the membranous septum, found adjacent to the septal leaflet of the tricuspid valve, and sometimes extend into the surrounding regions [Figure 15]. This defect results in fibrous continuity between the tricuspid and the

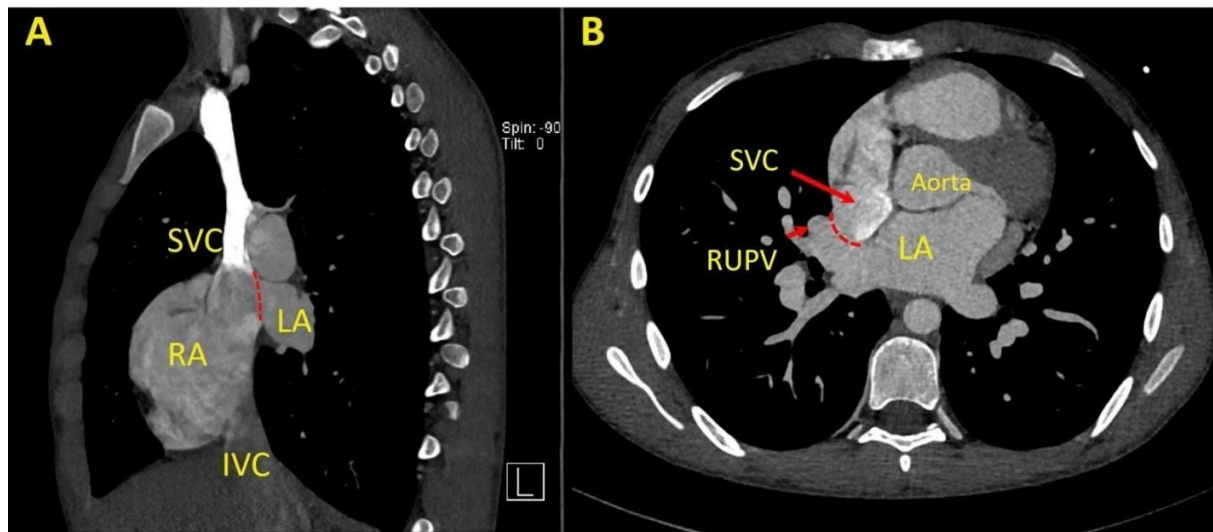


Figure 13. Panel A shows a still sagittal image from a cardiac computational tomography in a young adult imaging showing an absent wall (dotted red line) between the superior vena cava (SVC) and the left atrium (LA). Panel B shows a still axial image with the deficient wall between the SVC and the right upper pulmonary vein entrance (RUPV) (dotted red line) in a superior vena caval type sinus venosus defect. LA: Left atrium; RA: right atrium; IVC: inferior vena cava.

aortic valve (right and non-coronary) leaflets. The conduction system usually courses postero-inferior to the defect^[37,38].

Inlet ventricular septal defect

Inlet VSDs are the defects on the inlet portion of the tricuspid valve adjacent to the tricuspid septal leaflet and account for about 5% of VSDs. These are distinct from the atrioventricular septal defects as these have distinct tricuspid and mitral valves, and there is an absence of a common atrioventricular junction. Malalignment of the atrial and postero-inferior muscular ventricular septum results in straddling of the tricuspid valve^[3].

Muscular ventricular septal defect

These are also called trabecular muscular VSDs and are the second most common VSDs and have muscular borders. These are very common during fetal and neonatal life and most close spontaneously. Multiple muscular VSDs result in “Swiss-cheese” interventricular septum that is associated with significant interventricular shunting^[39,40] [Figure 16].

Outlet ventricular septal defect

Outlet VSDs may or may not be associated with malalignment. These are also called Doubly committed juxta-arterial VSD [Figure 17]. Although they are rare and account for ~5% of the VSDs, their prevalence is higher in patients of Asian heritage. Due to the underdevelopment or absence of the conal septum, this results in direct fibrous continuity between the aortic and pulmonary valves. Lack of supporting structure below the right coronary cusp results in prolapse and ultimate development of aortic regurgitation. Outlet VSDs with malalignment result in crowding and stenosis of the respective semilunar valves and resultant hypoplasia of downstream structures^[11,37].

ASSOCIATED LESIONS

It is not uncommon to have associated cardiac lesions along with simple septal defects. Common associated lesions include bicuspid aortic valve, additional atrial or ventricular septal defects, patent ductus arteriosus,

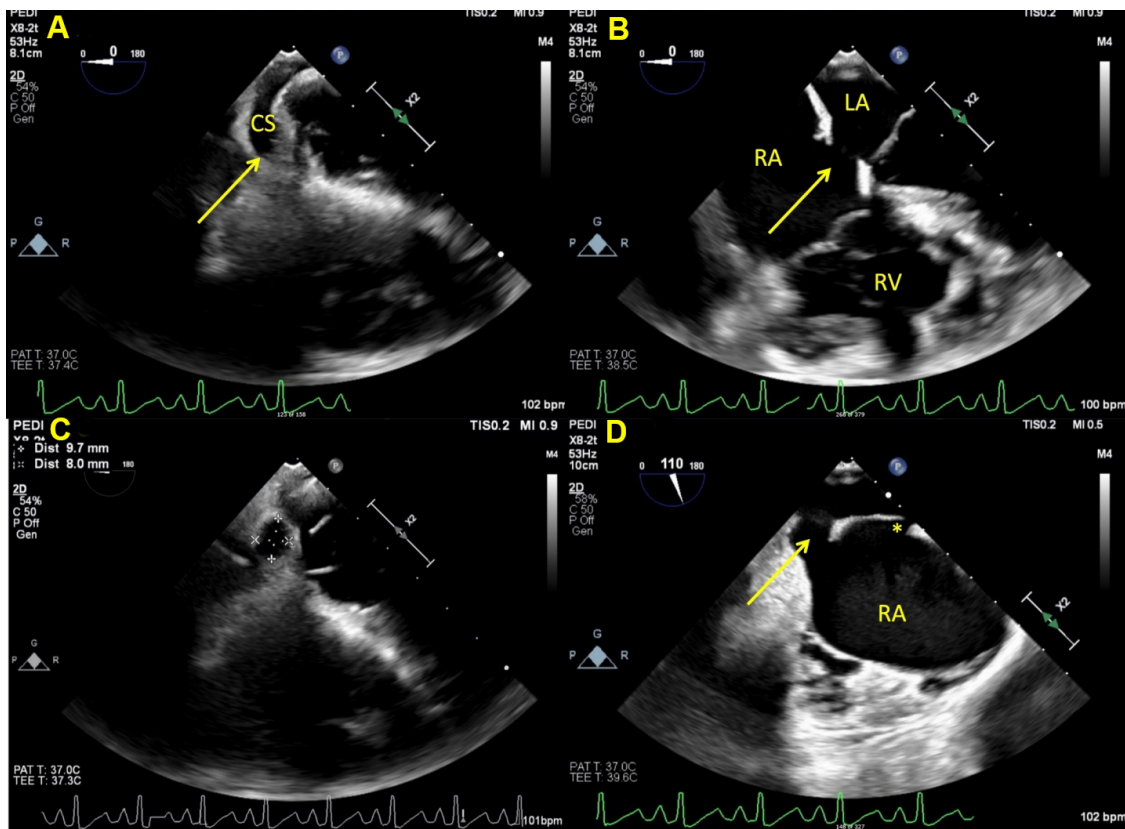


Figure 14. Still image from a trans-esophageal echocardiogram in a young child showing a coronary sinus defect (yellow arrow) in various views. Panel A shows the length of the coronary sinus at the level of the diaphragm. Panel B shows the CSD (yellow arrow) where the atrial septum around the CS ostium is deficient. Due to the proximity of this defect to the posterior portion of the tricuspid and mitral valve, it is not amenable to device closure. Panel C shows en face view of the CSD with measurements. Panel D shows the CSD (yellow arrow) in the midesophageal bicaval view when the probe is rotated leftward. There is an additional patent foramen ovale seen superiorly (asterisk). RA: Right atrium; LA: left atrium; CS: coronary sinus; CSD: coronary sinus defect.

right aortic arch, pulmonary valve stenosis. Development of subaortic membrane or double-chambered right ventricle due to hypertrophied muscle bundles can occur later in life and can recur post-operatively as well [Figures 18 and 19]. Aortic regurgitation can develop in perimembranous and outlet VSDs^[41]. Infective endocarditis is a potential risk and can occur even with small hemodynamically insignificant VSDs^[10,42].

IMAGING VENTRICULAR SEPTAL DEFECT

Given the complexity of ventricular septal development and anatomy, understanding the septal configuration is paramount in identifying the VSDs. In patients with good acoustic windows, all the intracardiac information can be obtained using 2D TTE. Reviewers can create a mental 3D map of the defect by incorporating slow, long echocardiographic sweeps and visualization of the defect from multiple views, which aids in understanding the defect, its relation to the surrounding structures and identifying associated lesions. Associated valvar problems, as in tricuspid or aortic regurgitation, can be identified by TTE. Thus, there is a role for 3D echocardiography in patients with good echocardiographic windows and sometimes can be helpful in patients undergoing device placement^[5,6].

There is a role for cross-sectional imaging using CMR or CT in patients with poor acoustic windows or complex VSDs. They are also superior in identifying vascular or non-cardiac structural problems. TEE might be used in carefully selected subjects based on the clinical question^[13,23,43].

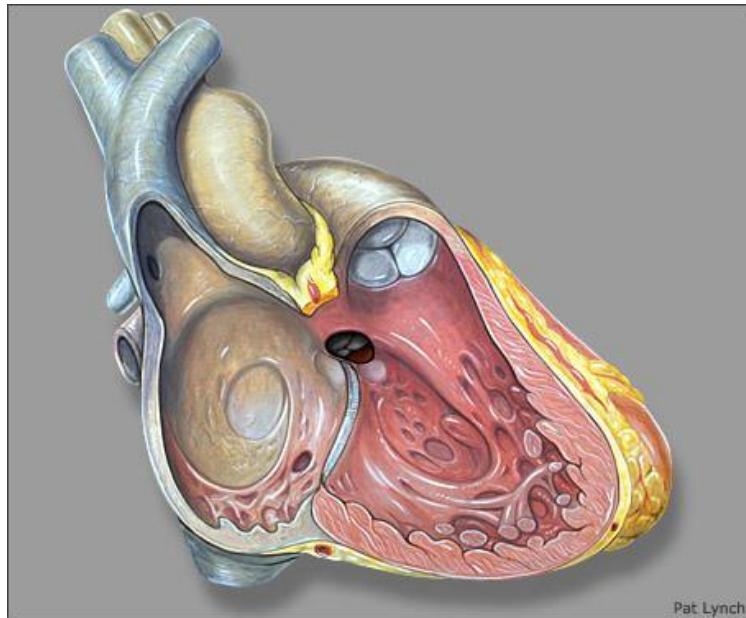


Figure 15. Image showing the perimembranous ventricular septal defect. The defect is located adjacent to the antero-septal commissure of the tricuspid valve.

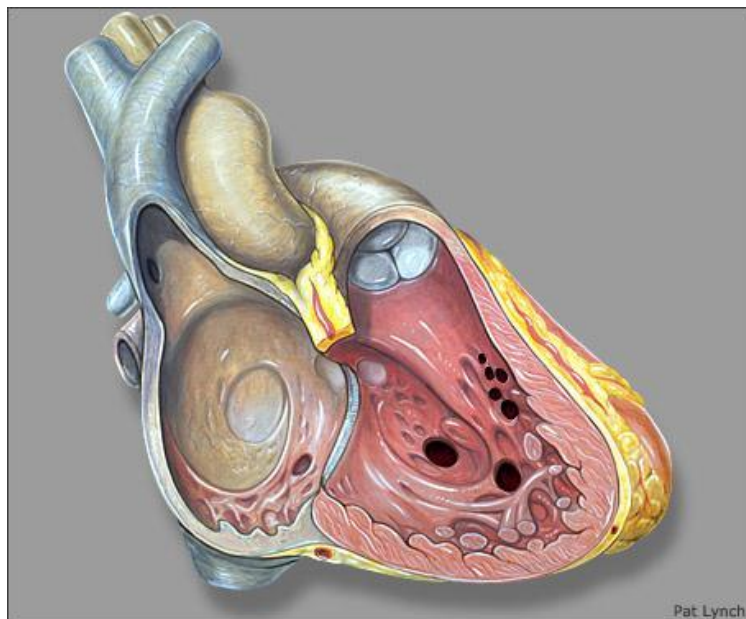


Figure 16. Image showing muscular ventricular septal defects at various possible locations in the trabecular portion of the interventricular septum.

Echocardiography also helps with identifying the direction of shunting using Doppler color flow mapping techniques. The Doppler left to right shunt gradient can help estimate right ventricular systolic pressure. The degree of left to right shunting across the VSD can be assessed based on the dilatation of the left-sided structures. The echocardiographic estimation of Q_p/Q_s using pulsed-wave Doppler-derived velocity time integral and calculated surface area across the outflow of interest technique has been proposed. However, its practical applicability in routine clinical practice is questionable due to various involved assumptions and

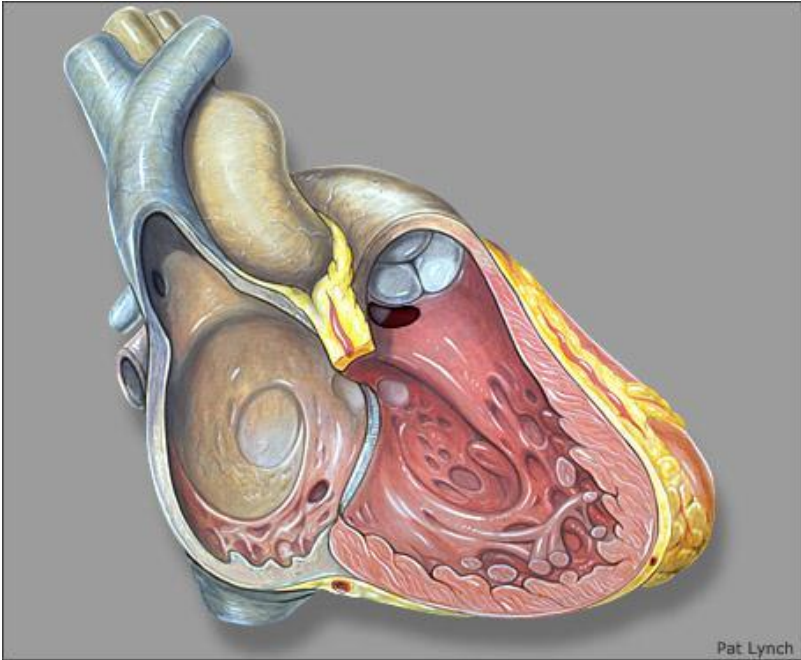


Figure 17. Image showing outlet ventricular septal defect. The defect is located below the pulmonary valve.

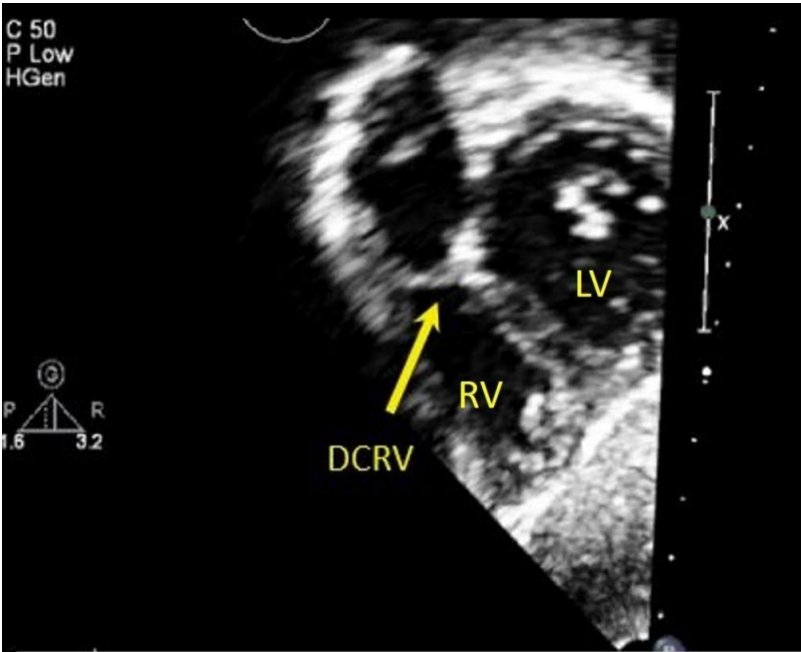


Figure 18. Still trans-thoracic echocardiogram in an infant in subcostal short axis showing a discrete membrane (arrow) within the right ventricular outflow tract resulting in a double-chambered right ventricle (DCRV). RV: Right ventricle; LV: left ventricle.

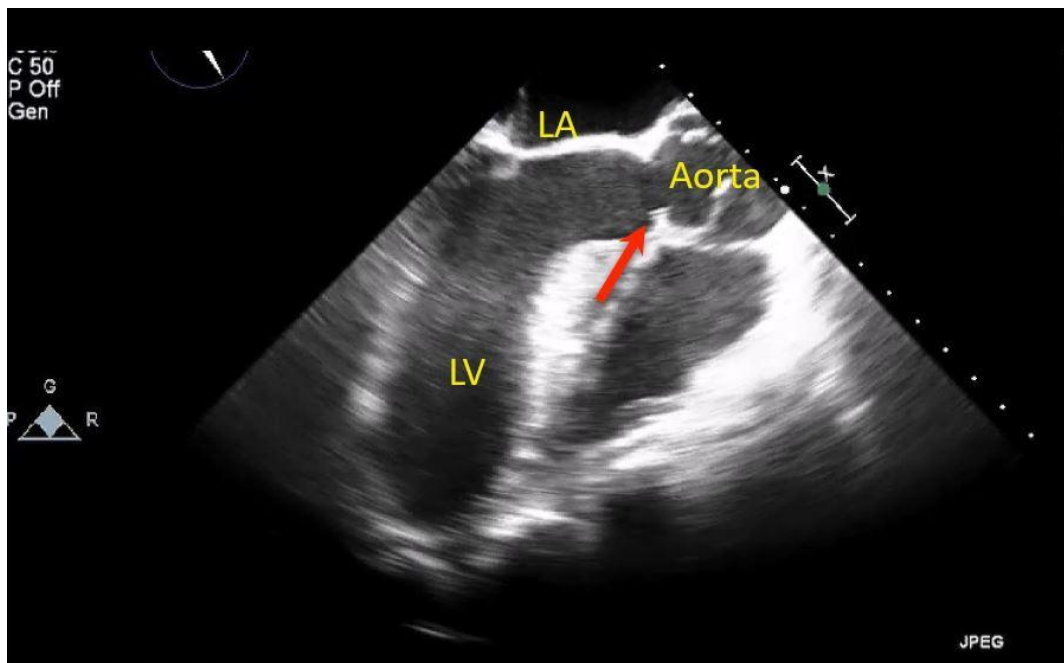


Figure 19. Still trans-esophageal echocardiogram in a young child in long-axis view showing a discrete membrane (red arrow) within the left ventricular outflow tract below the aortic valve. LA: Left atrium; LV: left ventricle.

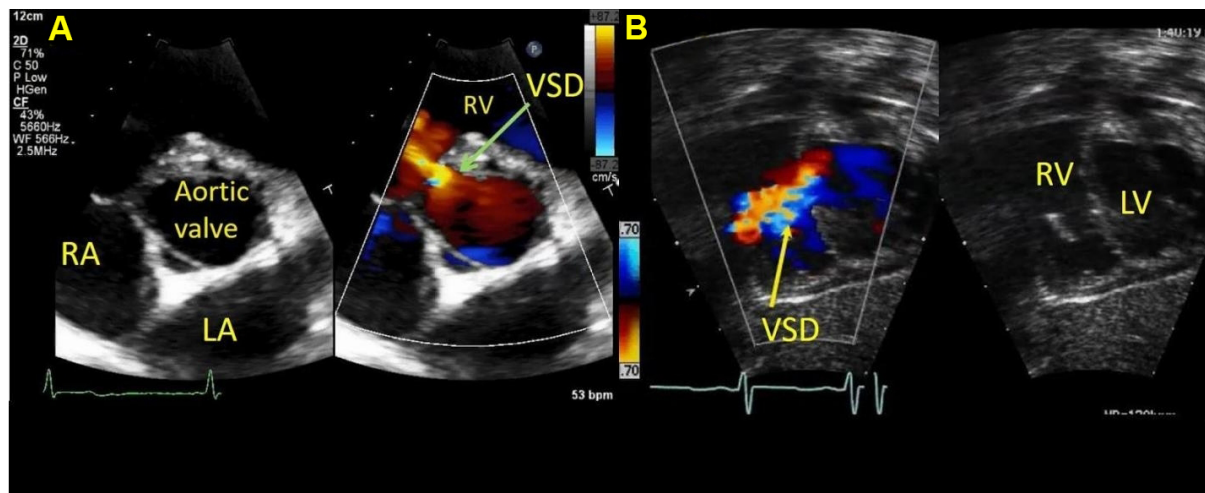


Figure 20. Still color Doppler image in a young child from a trans-thoracic echocardiogram in parasternal short axis (panel A) and Subcostal short axis (panel B) showing the perimembranous ventricular septal defect (VSD) with the left to right shunting by color Doppler (arrow). RA: Right atrium; LA: left atrium; RV: right ventricle; LV: left ventricle.

tends to overestimate the degree of left to right shunting compared to catheterization derived Q_p/Q_s ^[9,44-46].

Perimembranous VSDs are located adjacent to the antero-septal commissure of the tricuspid valve and can be assessed from the parasternal views, apical views, subcostal short axis and right anterior oblique views, which can be obtained by rotating the transducer counter-clockwise 45 degrees from subcostal long-axis view, this is a very good imaging plane as it shows the inlet and outlet portions simultaneously along with better visualization of the conal septum and right ventricular outflow tract [Figure 20]. It is important to

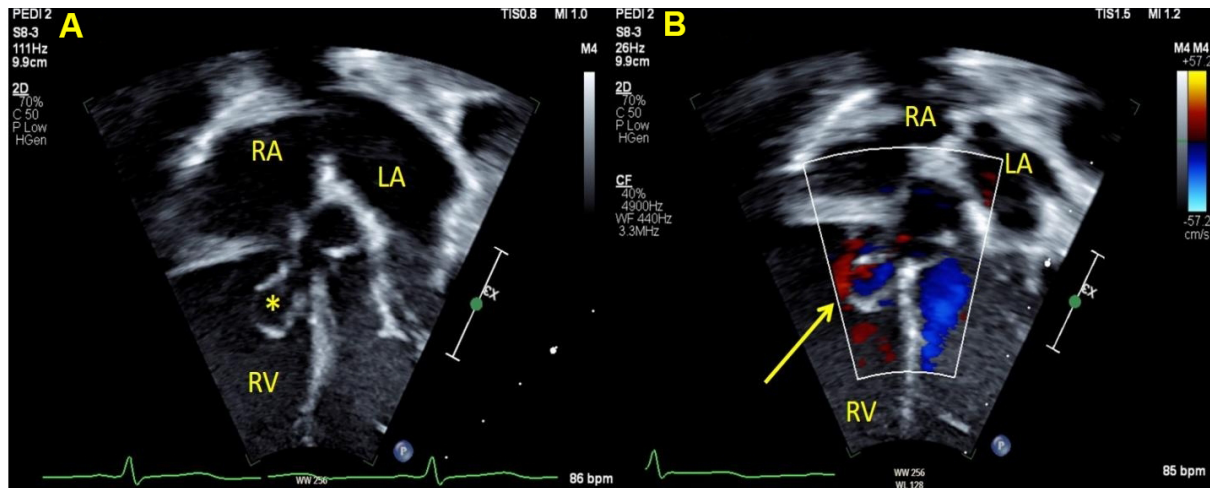


Figure 21. Still color compare image in a young child from a trans-thoracic echocardiogram in apical modified 4-chamber view showing perimembranous ventricular septal defect with left to right shunting by color Doppler. The left to right shunt is restricted due to the membranous aneurysm formed from the septal leaflet of the tricuspid valve (asterisk and arrow). RA: Right atrium; LA: left atrium; RV: right ventricle.

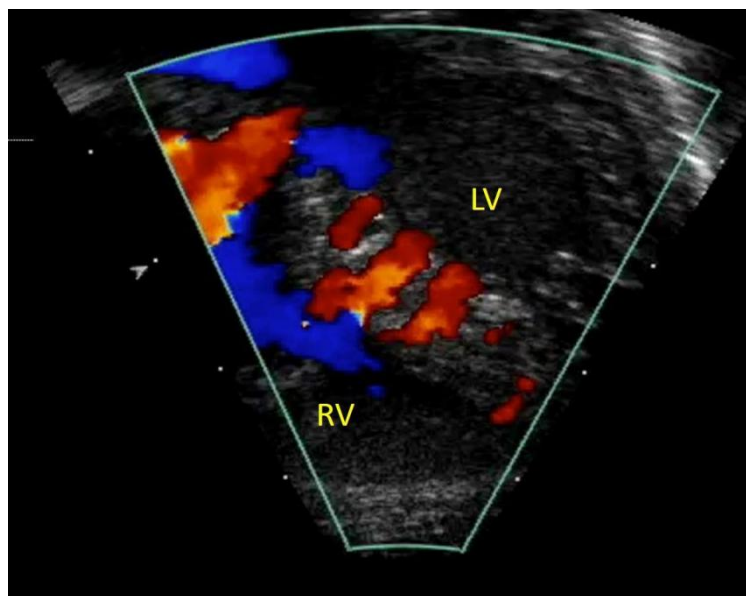


Figure 22. Still color Doppler image in a teenager from a trans-thoracic echocardiogram in modified apical four-chamber view showing multiple muscular ventricular septal defects with the left to right shunting. RV: Right ventricle; LV: left ventricle.

evaluate tricuspid valve function as it is immediately adjacent to the defect. The septal leaflet of the tricuspid valve may grow into a pouch over time, resulting in a so-called “membranous aneurysm” that over time restricts the degree of left to right shunting [Figure 21]. In addition, the aortic right and non-coronary cusps are directly above the defect and sometimes may prolapse into the defect due to lack of support and high-velocity VSD shunting that creates a low-pressure zone that impacts the aortic valve function and thus resulting in new aortic regurgitation^[3,41].

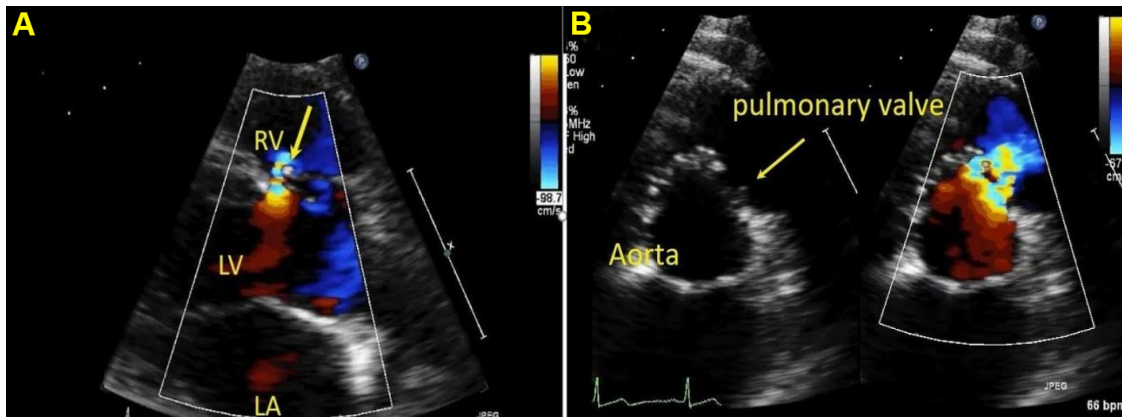


Figure 23. Still color compare image from a trans-thoracic echocardiogram in a young adult in the parasternal long axis (panel A) and parasternal short axis (panel B) showing outlet ventricular septal defect (VSD) with the left to right shunting by color Doppler (arrow). Color flow is directed towards the pulmonary valve. LA: Left atrium; RV: right ventricle; LV: left ventricle.

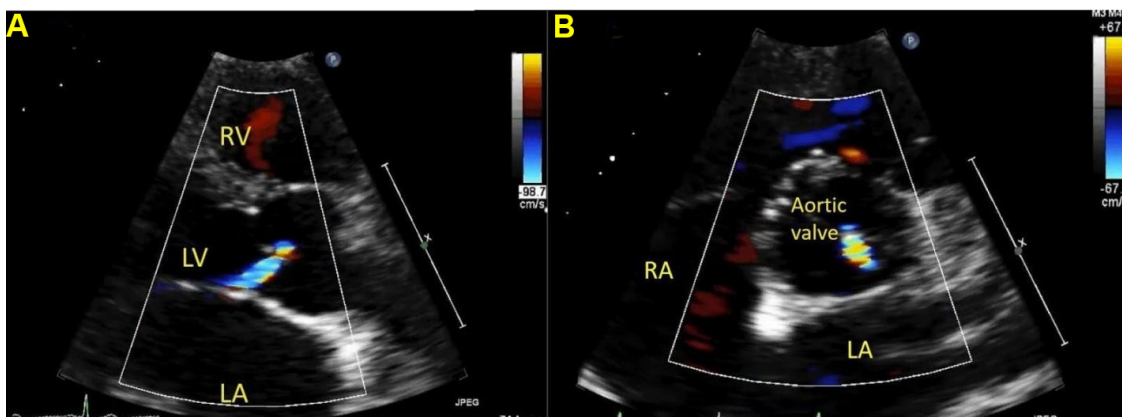


Figure 24. Still color image from a trans-thoracic echocardiogram in a young child in the parasternal long axis (panel A) and parasternal short axis (panel B) showing aortic regurgitation in a patient with outlet ventricular septal defect in diastole. Regurgitation flow is directed posteriorly towards the anterior mitral leaflet. RA: Right atrium; LA: left atrium; RV: right ventricle; LV: left ventricle.

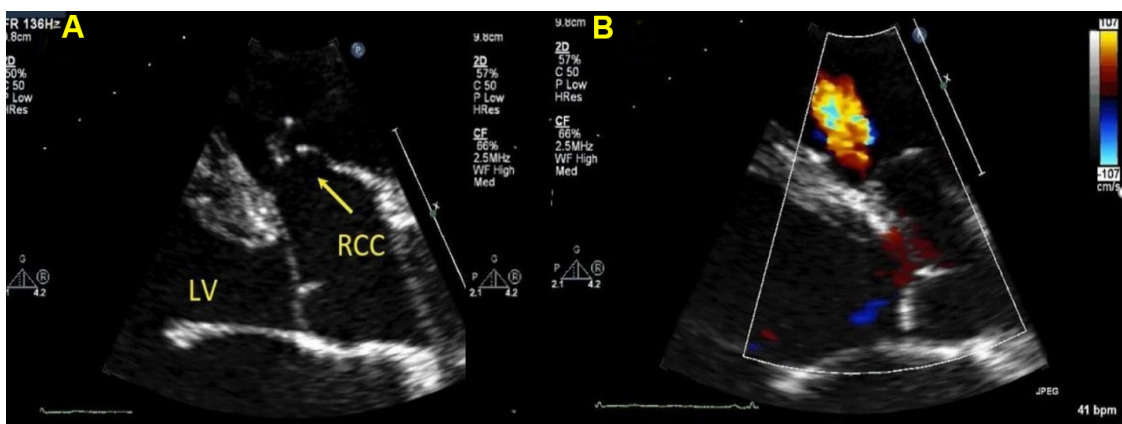


Figure 25. Still color compare image from a trans-thoracic echocardiogram in a young adult in parasternal long axis panel A shows elongated aneurysmal right coronary cusp that is sucked into the outlet ventricular septal defect consistent with sinus of valsalva aneurysm. Panel B shows the same image with the color flow, VSD jet is seen as red. RCC: Right coronary cusp; LV: left ventricle.

One has to be careful when assessing muscular VSDs as there can be multiple defects, and thus imaging from modified apical view making the interventricular septum perpendicular to the ultrasound probe and slowly sweeping the septum can help [Figure 22].

Outlet VSDs are seen as defects between 12 and 3 o'clock when visualized in the parasternal short-axis views with color flow directed towards the right ventricular outflow and pulmonary valve. They are at higher risk for developing aortic valve prolapse and aortic regurgitation. As such, this has to be carefully assessed at follow-up visits^[41]. Aneurysm of the sinus of Valsalva has also been described with outlet VSDs that can progress over time [Figures 23-25].

CONCLUSION

Atrial and ventricular septal defects can occur in isolation or associated with other CHDs; together, they account for the majority of the CHDs. Therefore, knowledge of septal embryology and anatomy is crucial to understanding these lesions along with planning interventions. In addition, it is important to identify associated lesions and potential complications. This chapter reviews various noninvasive imaging modalities and how they can be utilized for these lesions.

DECLARATIONS

Acknowledgments

The author would like to thank Patrick Lynch for allowing the author to use his beautiful images.

Authors' contributions

The author contributed solely to the article.

Availability of data and materials

Not applicable.

Financial support and sponsorship

None.

Conflicts of interest

The author declared that there are no conflicts of interest.

Ethical approval and consent to participate

Not applicable.

Consent for publication

Not applicable.

Copyright

© The Author(s) 2022.

REFERENCES

1. Liu Y, Chen S, Zühlke L, et al. Global birth prevalence of congenital heart defects 1970-2017: updated systematic review and meta-analysis of 260 studies. *Int J Epidemiol* 2019;48:455-63. DOI PubMed PMC
2. Keane JF, Geva T, Fyler DC. Atrial septal defect. second. In: Keane JF, Lock JE, Fyler DC, editors. *Nadas' pediatric cardiology*. second. Philadelphia: Saunders; 2006. p. 603-16.
3. Natarajan S, Cohen MS. Ventricular septal defects. 2nd ed. In: Lai WW, Mertens LL, Cohen MS, Geva T, editors. *Echocardiography in pediatric and congenital heart disease: from fetus to adult*. 2nd ed. Oxford, UK: John Wiley & Sons, Ltd; 2016. p. 215-30.

4. Redington AN, Anderson RH, Spicer DE. Interatrial communications. 4th ed. In: Wernovsky G, editor. *Anderson's pediatric cardiology*. 4th ed. Elsevier, Inc.; 2019. p. 503-15.
5. Tretter JT, Benson L, Crucean A, Spicer DE, Anderson RH. Ventricular septal defect. 4th ed. In: Wernovsky G, editor. *Anderson's pediatric cardiology*. 4th ed. Elsevier, Inc.; 2019. p. 555-84.
6. Sachdeva R. Atrial septal defects. 9th ed. In: Allen HD, Shaddy RE, Penny DJ, Feltes TF, Cetta F, editors. *Moss and Adams' heart disease in infants, children, and adolescents: including the fetus and young adult*. 9th ed. Philadelphia, PA 19103: Lippincott Williams & Wilkins; 2016.
7. Geva T. Anomalies of the atrial septum. 2nd ed. In: Lai WW, Mertens LL, Cohen MS, Geva T, editors. *Echocardiography in pediatric and congenital heart disease: from fetus to adult*. 2nd ed. Oxford, UK: John Wiley & Sons, Ltd; 2016. p. 197-214.
8. Uppu SC, Rao PS. Secundum atrial septal defect closure. In: Mahadevan VS, editor. *Textbook of interventions in adult congenital heart disease a case-based approach*. Springer International Publishing; 2021.
9. Pushparajah K. Non-invasive Imaging in the Evaluation of Cardiac Shunts for Interventional Closure. *Front Cardiovasc Med* 2021;8:651726. [DOI](#) [PubMed](#) [PMC](#)
10. Stout KK, Daniels CJ, Aboulhosn JA, et al. 2018 AHA/ACC Guideline for the management of adults with congenital heart disease: executive summary: a report of the American College of Cardiology/American Heart Association Task Force on clinical practice guidelines. *Circulation* 2019;139:e637-97. [DOI](#) [PubMed](#)
11. Lopez L, Houyel L, Colan SD, et al. Classification of ventricular septal defects for the eleventh iteration of the international classification of diseases-striving for consensus: a report from the international society for nomenclature of paediatric and congenital heart disease. *Ann Thorac Surg* 2018;106:1578-89. [DOI](#) [PubMed](#)
12. Sadler TW. *Langman's medical embryology*. 14th ed. Philadelphia: Lippincott Williams & Wilkins; 2018.
13. Patel MD. Atrial septal defects, ventricular septal defects, atrioventricular septal defects, and unroofed coronary sinus. In: Adebo DA, editor. *Pediatric cardiac CT in congenital heart disease*. Cham: Springer International Publishing; 2021. p. 55-62. [DOI](#)
14. Geva T. Abnormal Systemic Venous Connections. 9th ed. In: Allen HD, Shaddy RE, Penny DJ, Feltes TF, Cetta F, editors. *Moss and Adams' heart disease in infants, children, and adolescents: including the fetus and young adult*. 9th ed. Philadelphia, PA 19103: Lippincott Williams & Wilkins; 2016. p. 911-33.
15. Gandy K, Hanley F. Management of systemic venous anomalies in the pediatric cardiovascular surgical patient. *Semin Thorac Cardiovasc Surg Pediatr Card Surg Annu* 2006;63-74. [DOI](#) [PubMed](#)
16. Webb G, Gatzoulis MA. Atrial septal defects in the adult: recent progress and overview. *Circulation* 2006;114:1645-53. [DOI](#) [PubMed](#)
17. Goldberg DJ. *Atrial Septal Defects. Fetal cardiovascular imaging a disease-based approach*. Philadelphia, PA: Elsevier/Saunders; 2012. p. 98-101.
18. Lopez L, Chambers S. Systemic venous anomalies. In: Lai WW, Mertens LL, Cohen MS, Geva T, editors. *Echocardiography in pediatric and congenital heart disease*. Oxford: John Wiley & Sons, Ltd; 2016. p. 180-96.
19. Raghil G, Ruttenberg HD, Anderson RC, Amplatz K, Adams P Jr, Edwards JE. Termination of left superior vena cava in left atrium, atrial septal defect, and absence of coronary sinus: a developmental complex. *Circulation* 1965;31:906-18. [DOI](#) [PubMed](#)
20. Xie MX, Yang YL, Cheng TO, et al. Coronary sinus septal defect (unroofed coronary sinus): echocardiographic diagnosis and surgical treatment. *Int J Cardiol* 2013;168:1258-63. [DOI](#) [PubMed](#)
21. Rao PS, Harris AD. Recent advances in managing septal defects: atrial septal defects. *F1000Res* 2017;6:2042. [DOI](#) [PubMed](#) [PMC](#)
22. Shirali GS, Simpson J. Three-dimensional echocardiography. 4th ed. In: Wernovsky G, editor. *Anderson's pediatric cardiology*. 4th ed. Elsevier, Inc.; 2019. p. 309-16.
23. Budts W, Miller O, Babu-Narayan SV, et al. Imaging the adult with simple shunt lesions: position paper from the EACVI and the ESC WG on ACHD. Endorsed by AEPC (Association for European Paediatric and Congenital Cardiology). *Eur Heart J Cardiovasc Imaging* 2021;22:e58-70. [DOI](#) [PubMed](#)
24. Johnson TR, Fogel MA. Abnormalities of the atria and systemic veins. In: Fogel MA, editor. *Principles and practice of cardiac magnetic resonance in congenital heart disease: form, function, and flow*. Oxford, UK: Wiley-Blackwell; 2010. p. 110-23. [DOI](#)
25. Ostermayer SH, Srivastava S, Doucette JT, et al. Malattached septum primum and deficient septal rim predict unsuccessful transcatheter closure of atrial communications. *Catheter Cardiovasc Interv* 2015;86:1195-203. [DOI](#) [PubMed](#)
26. Rao PS. Transcatheter closure of complex atrial septal defects. *Echocardiography* 2014;31:1173-6. [DOI](#) [PubMed](#)
27. Rosenfeld HM, van der Velde ME, Sanders SP, et al. Echocardiographic predictors of candidacy for successful transcatheter atrial septal defect closure. *Cathet Cardiovasc Diagn* 1995;34:29-34. [DOI](#) [PubMed](#)
28. Mallula K, Amin Z. Recent changes in instructions for use for the Amplatzer atrial septal defect occluder: how to incorporate these changes while using transesophageal echocardiography or intracardiac echocardiography? *Pediatr Cardiol* 2012;33:995-1000. [DOI](#) [PubMed](#)
29. Damodaran S, Gourav KP, Negi S, Halder V, Azmeera S. Giant Eustachian valve and Thebesian valve - a highly deceptive structures as atrial septal defect rims. *J Clin Ultrasound* 2021;49:506-8. [DOI](#) [PubMed](#)
30. Raut MS, Maheshwari A, Dubey S, Shivnani G, Makhija A, Mohanty A. Eustachian valve - masquerading ASD rim. *Indian Heart J* 2016;68:368-9. [DOI](#) [PubMed](#) [PMC](#)
31. Krishnamoorthy KM, Gopalakrishnan A, Kumar DS, Sivasankaran SS. Eustachian valve - masquerading ASD rim. *Indian Heart J* 2017;69:422-3. [DOI](#) [PubMed](#) [PMC](#)

32. Jone PN, Haak A, Ross M, et al. Congenital and structural heart disease interventions using echocardiography-fluoroscopy fusion imaging. *J Am Soc Echocardiogr* 2019;32:1495-504. DOI PubMed
33. Hansen JH, Duong P, Jivanji SGM, et al. Transcatheter correction of superior sinus venosus atrial septal defects as an alternative to surgical treatment. *J Am Coll Cardiol* 2020;75:1266-78. DOI PubMed
34. Cohen MS, Lopez L. Ventricular septal defects. 9th ed. In: Allen HD, Shaddy RE, Penny DJ, Feltes TF, Cetta F, editors. Moss and Adams' heart disease in infants, children, and adolescents: including the fetus and young adult. 9th ed. Philadelphia, PA 19103: Lippincott Williams & Wilkins; 2016.
35. Thacker D, Goldberg DJ. Ventricular Septal Defects. Fetal cardiovascular imaging a disease-based approach. Philadelphia, PA: Elsevier/Saunders; 2012. p. 83-95.
36. Soto B, Becker AE, Moulart AJ, Lie JT, Anderson RH. Classification of ventricular septal defects. *Br Heart J* 1980;43:332-43. DOI PubMed PMC
37. Spicer DE, Hsu HH, Co-Vu J, Anderson RH, Fricker FJ. Ventricular septal defect. *Orphanet J Rare Dis* 2014;9:144. DOI PubMed PMC
38. Keane JF, Fyler DC. Ventricular septal defect. second. In: Keane JF, Lock JE, Fyler DC, editors. Nadas' pediatric cardiology. second. Philadelphia: Saunders; 2006. p. 527-48.
39. Rao PS, Harris AD. Recent advances in managing septal defects: ventricular septal defects and atrioventricular septal defects. *F1000Res* 2018;7:498. DOI PubMed PMC
40. Praagh S, Mayer JE, Berman NB, Flanagan MF, Geva T, Van Praagh R. Apical ventricular septal defects: follow-up concerning anatomic and surgical considerations. *Ann Thorac Surg* 2002;73:48-56. DOI PubMed
41. Tweddell JS, Pelech AN, Frommelt PC. Ventricular septal defect and aortic valve regurgitation: pathophysiology and indications for surgery. *Semin Thorac Cardiovasc Surg Pediatr Card Surg Annu* 2006:147-52. DOI PubMed
42. Berglund E, Johansson B, Dellborg M, et al. High incidence of infective endocarditis in adults with congenital ventricular septal defect. *Heart* 2016;102:1835-9. DOI PubMed
43. Printz BF. Abnormalities of the ventricles and pericardium. In: Fogel MA, editor. Principles and practice of cardiac magnetic resonance in congenital heart disease: form, function, and flow. Oxford, UK: Wiley-Blackwell; 2010. p. 124-54. DOI
44. Kitabatake A, Inoue M, Asao M, et al. Noninvasive evaluation of the ratio of pulmonary to systemic flow in atrial septal defect by duplex Doppler echocardiography. *Circulation* 1984;69:73-9. DOI PubMed
45. Dittmann H, Jacksch R, Voelker W, Karsch K, Seipel L. Accuracy of doppler echocardiography in quantification of left to right shunts in adult patients with atrial septal defect. *J Am Coll Cardiol* 1988;11:338-42. DOI PubMed
46. Sanders SP, Yeager S, Williams RG. Measurement of systemic and pulmonary blood flow and QP/QS ratio using doppler and two-dimensional echocardiography. *Am J Cardiol* 1983;51:952-6. DOI PubMed